Proceedings, 5th AOSFST, Newcastle, Australia, 2001
Editors: M.A. Delichatsios, B.Z. Dlugogorski and E.M. Kennedy

EXPERIMENTAL FLAME CORRELATIONS AND DIMENSIONAL RELATIONS IN TURBULENT CEILING FIRES

Y. Hasemi[a], and D. Nam[a] and M. Yoshida[b]

a. Department of Architecture, Waseda University

b. National Institute of Land, Infrastructure Management

JAPAN

ABSTRACT

Flame size and heat flux correlations were obtained by experiments for circular turbulent flame sheets developing from a downward injection source beneath an unconfined inert ceiling, and are compared against those for one-dimensional ceiling flames. These correlations show proportionality of the flame sheet area to heat release rate and the representation of flame heat transfer as a function of the distance from the source normalised by flame length. Heat release rate per unit flame sheet area in circular flames is found to be significantly smaller than that in one-dimensional flames. It suggests a weaker entrainment of ambient air to circular flames than to one-dimensional flames. Total heat flux to the ceiling surface from the flame sheet is less than 30 kW/m^2 and is not enough to accelerate flame spread. This suggests the importance of preheating of a combustible ceiling by a hot gas layer for the fast fire spread generally observed in real and experimental room fires. Dimensional analysis based on the experimental results suggests the proportionality of horizontal velocity to the distance from the upstream end of the burning surface, and faster velocity in one-dimensional flames than in circular flames.

Keywords: Ceiling fire, flame length, heat flux, heat release rate, dimensional analysis.

INTRODUCTION

Flame development under a ceiling is very often the direct trigger for the occurrence of flashover during a compartment fire. Experiments have also reported interesting features of ceiling fires including formation of cellular laminar flames due to local convection[1], significant change of total flame length after the start of flame development beneath a ceiling in compartment fires[2,3], etc. In spite of the importance of ceiling fires for fire safety, few works have been conducted on the prediction of the properties of ceiling flames. While Froude modeling has been applied successfully to "vertical" turbulent flames in fires[4,5,6,7], it is important that buoyancy is not the driving force for a flame flow beneath a ceiling. Many experiments have been conducted on turbulent upward flames impinging on a ceiling. However, it is still difficult to understand the controlling mechanism of the "ceiling flame" part of such flames. In order to seek the controlling mechanism of ceiling flames, the authors produced one-dimensional "pure ceiling flames" beneath an inert ceiling using a downward channel with water-cooled side walls for the simplicity of the analysis and

reported proportionality of the flame area to heat release rate[8]. During examination of previous works on flame impingement to the ceiling, a sign was found that horizontal flame development beneath the ceiling can be highly dependent on the mode of flame development whether it is one-dimensional or two dimensional. This study intends to report experiments on circular flames beneath an inert ceiling and to compare the results with those from previous experiments on one-dimensional ceiling fires. This paper also tries to discuss dimensional relations in excess temperature, velocity and flame thickness as a basis for developing a more quantitative model of ceiling flames.

EXPERIMENTAL

An inert unconfined ceiling was produced with two layers of 12 mm thick 1820 mm long square mineral fiber boards, and a steel cylindrical porous burner was installed at the center of the ceiling with the injection surface downward flush to the ceiling (Figure 1). No soffit was attached. Two burners of different diameters, 90 mm and 160 mm, were prepared to examine the fuel size effect. The burner was filled with 5 mm diameter ceramic balls and its injection surface was covered by stainless wire mesh. Propane (commercial) was used as the fuel. In the preliminary tests it had been confirmed that ceiling flames start to flood from the edge of the present ceiling at the nominal heat release rate around 100 kW. Hence, measurements were carried out for the range of nominal heat release rates from 5 kW to 80 kW.

In order to measure heat flux to the ceiling surface, ten Schmidt-Boelter 100 kW/m^2 range heat flux gages (15 mm diameter) were inserted downward to the ceiling at intervals of 100 mm for the first 6 gages from the center, and 150 mm for the remainder. Fuel supply rate was monitored with a gas flow meter, and the flame geometry was recorded by digital-video. The reported flame radius is the average over 1 min of the data recorded at 1 s intervals. The whole apparatus was built beneath a smoke collection hood. Heat release measurements were conducted in the smoke exhaust duct by the oxygen consumption method. The heat release rate thus measured will be referred to as effective heat release rate. The shape of these flames was quite sensitive to accidental disturbance; even a trifling inclination of the ceiling was found to make an “egg-shaped” flame pointed toward the upward direction. The level of the ceiling surface and the coincidence of the surfaces of the ceiling and the burner were confirmed in every test. However, even weak and accidental draft within the laboratory was found to make more than 10% difference between the windward and the leeward radii. The reported flame radius and flame heat flux were obtained only while establishment of exact circular flames was confirmed. No measurement was conducted on the temperature and velocity profiles. A simple visualisation of the flow beneath the flame sheet was conducted by introducing incense smoke through a Teflon tube.

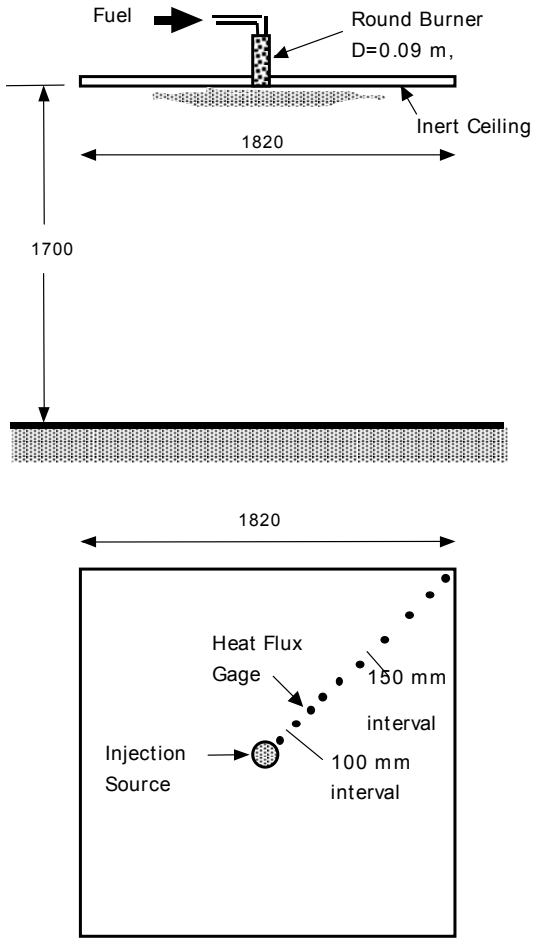

Figure 1: Experimental setup.

EXPERIMENTAL RESULTS

The digital data are summarised in Table 1. The reported nominal heat release rates were calculated from fuel gas supply rates assuming complete combustion. While the experiments were conducted by increasing the nominal heat release rate from 5 kW with the interval of 5 kW, the flame for 5 kW looked like a cluster of cellular laminar flamelets around the injection source. The present paper deals only with the results at 10 kW and larger, where steadily spreading radial turbulent flame was observed. Flame behaviour in these conditions is believed to be dominated by the inertial force far more strongly than the case studied by Orloff and de Ris[1]. It is also noteworthy that the effective heat release rate was significantly smaller than the nominal one as seen in Table 1. Similar results were also seen in the one-dimensional flame sheet in a downward horizontal channel[8]. These results suggest significant decrease of the combustion efficiency in a concurrent flame spread beneath a downward horizontal surface. While most previous experiments on the deterministic flame properties represent the source intensity by a nominal heat release rate, the following analysis will use effective heat release rate as it is believed to affect more directly the flame behaviour.

Table 1: Summary, digital experimental data.

(a) Burner diameter = 90 mm

Nominal Heat Release Rate (kW)		10	20	30	40	50	60	70	80
Effective Heat Release Rate (kW)		3.0	8.3	10.5	15.7	16.9	25.2	31.8	38.1
Flame Radius (m)		0.225	0.375	0.5	0.55	0.65	0.75	0.85	0.90
Total heat flux (kW/m^2)	R = 0.10 (m)	18.9	23.7	24.8	26.3	27.0	26.7	26.6	25.0
	0.20	12.1	13.3	16.3	18.4	19.1	17.8	20.6	19.8
	0.30	4.5	9.6	14.0	14.7	17.2	16.4	19.8	17.5
	0.40	2.3	4.5	8.5	11.6	12.1	11.1	14.5	14.7
	0.50	1.6	3.0	4.7	7.7	8.6	7.3	10.1	11.5
	0.60	0.9	1.9	2.9	5.0	5.6	5.1	7.9	8.6
	0.75	0.6	1.3	2.1	3.6	4.0	3.6	5.3	6.3
	0.90	0.3	0.7	1.2	2.1	2.3	2.6	3.2	3.7
	1.05	0.2	0.6	1.0	1.8	1.9	2.3	2.6	3.2
	1.20	0.2	0.3	0.6	1.3	1.4	1.6	1.8	2.2

(b) Burner diameter = 160 mm

Nominal Heat Release Rate (kW)		10	20	30	40	50	60	70	80
Effective Heat Release Rate (kW)		6	9.2	12	15.7	19.5	28.1	34.5	33.7
Flame Radius (m)		0.25	0.35	0.5	0.6	0.65	0.7	0.8	0.85
Total heat flux (kW/m^2)	R = 0.10 (m)	14.1	17.1	20.4	16.8	19.9	18.1	19.8	16.4
	0.20	9.2	13.2	15.2	14.2	16.6	16.9	16.0	15.8
	0.30	4.2	9.2	11.2	11.3	12.8	16.6	15.7	13.4
	0.40	2.3	4.5	9.1	9.7	10.8	11.3	12.6	11.5
	0.50	1.5	2.6	5.0	7.0	8.7	9.9	10.0	10.7
	0.60	0.9	1.8	3.3	4.0	5.5	6.8	7.8	8.4
	0.75	0.6	1.2	2.4	2.9	3.6	4.1	5.3	5.3
	0.90	0.3	0.6	1.4	1.9	2.2	2.7	3.1	3.3
	1.05	0.2	0.4	1.1	1.6	1.8	2.2	2.6	2.7
	1.20	0.2	0.3	0.8	1.2	1.3	1.6	1.8	2.0

Flame dimensions

Figure 2 represents the correlation between the flame radius and effective heat release rate. The flame sheet developed steadily beneath the ceiling, and apparently there was no systematic change of the flame thickness in the radial direction between $r = 0$ and $r = 0.5L_f$. Although occasional wave-like behaviour was seen along the flame sheet surface and the colour of the flame became thinner with increasing radial distance for approximately $r > 0.5L_f$, there was no such significant oscillation of the flame itself as normally seen in vertical flames. Simple visualisation with artificial smoke suggests the existence of vertical air flow toward the ceiling beneath the flame sheet. From this observation, significant horizontal flow along the ceiling is believed to exist only within the flame. This discontinuity of the flow pattern is probably because of the discontinuity of temperature that makes the ceiling flame a shear-free flow.

Figure 2: Relation between the radius of circular ceiling flame and effective heat release rate.

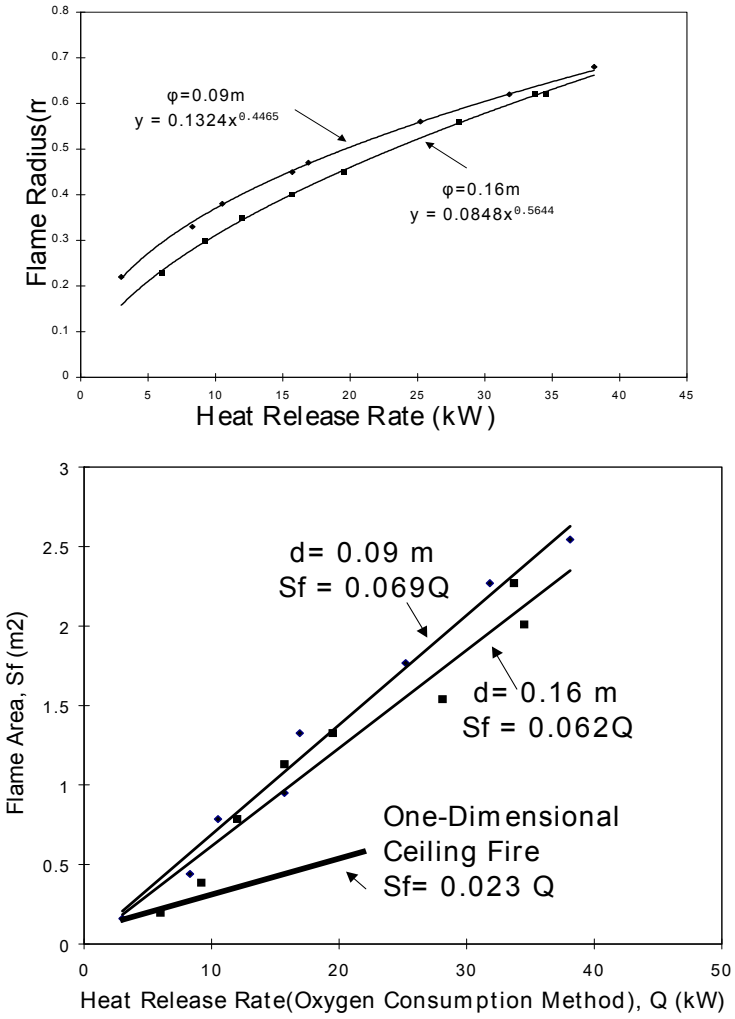

Figure 3: Area covered by ceiling flame vs. effective heat release rate.

The flame radius was slightly larger with the 90 mm burner than with the 160 mm burner. It is noteworthy that the two curves in Figure 2 are almost parallel to each other with the 90 mm burner curve around 2 kW left of the 160 mm burner curve, and the source size effect on the flame radius becomes insignificant with the increase of effective heat release rate. The larger flame radius for a smaller injection source suggests the tendency that entrainment is enhanced by the increase of size of the injection source. This is probably because the horizontal velocity near the injection source is blocked by the increase in the downward inertial force

of the fuel flow using a larger injection source. There was no clear dependence shown for the thickness of the flame sheet on heat release rate within the present range of heat release rates (nominal 10 – 80 kW). The power dependence seen in Figure 2, roughly $LQ^{1/2}$, suggests a proportionality of the flame sheet area to the heat release rate. Together with the similar proportionality already reported for one-dimensional ceiling flames[8], this suggests the uniformity of entrainment and local burning rate within a ceiling flame. Figure 3 is a summary of the relationship between the flame sheet area and effective heat release rate from the present and previous tests. It is interesting that the flame sheet area for circular flames is significantly larger than that for one- dimensional flames.

While the largest nominal heat release rate in the present tests was only 80 kW, the flame sheet radius with this heat input was 0.85 – 0.90 m; the corresponding flame sheet diameter, 1.7 – 1.8 m, is large enough to compare with the height of an adult man. This suggests significant dependence of the "size" of a flame on the configuration, because an unconfined nominal 80 kW fire above a floor makes only a 1.1 m tall turbulent flame[6]. Although it is difficult to compare the "size" of flames of different configurations, it is still believed that a 1.7 to 1.8 m diameter ceiling flame is significantly larger than a 1.1 m tall cylindrical flame above the floor. Many experiments report significant growth of flames beneath ceilings, perhaps due to this effect. The significant spread of a flame beneath a ceiling even for a relatively small heat input should also result in making a large radiation source against the floor and combustible objects above the floor. Importance of the control of the burning behaviour of a ceiling should be emphasised from this point of view.

Incident heat flux to ceiling

In previous experiments on wall and one-dimensional ceiling flames, it has been confirmed that flame heat transfer can be represented as a function of distance normalised by flame length[8,9]. From this experience, flame heat transfer has been correlated against distance from the center of the cylindrical burner divided by the flame radius. As seen in Figure 4, the results for the 90 mm diameter and 160 mm diameter burners are quite close, except at the center of the circular flames, where heat flux is slightly greater for the 90 mm burner than for the 160 mm burner.

The flame heat transfer rate is represented as:

$$r/L_f < 0.4 \qquad q_T \ 13.0(r/L_f)^{-1/3}$$

$$0.4 \ r/L_f < 0.7 \qquad q_T \ 7.0(r/L_f)^{-1}$$

$$0.7 \ r/L_f \qquad q_T \ 4.5(r/L_f)^{-2.2}$$

Comparison of the present results with those of other configurations[8,9] such as wall and one-dimensional ceiling flames leads to the following findings:

(1) The present heat transfer correlation against the normalised distance within the flame, $r/L_f < 1$, is very close to that for one-dimensional ceiling flames, whereas the present heat flux decays faster with distance than it does for one-dimensional flames.

(2) The present heat transfer is weaker than that for wall flames within the solid flame, $r/L_f < 0.7$, whereas the heat transfer for circular and one-dimensional ceiling flames is greater than that for wall flames in $r/L_f > 0.7$.

The weak heat flux within the flame sheet, less than 30 kW/m^2, may sound unexpectedly small if the fast fire spread along a ceiling in real and experimental fires is considered. This is probably because a ceiling flame tends to be thin due to the strong buoyancy effects. While it is difficult for such weak heat fluxes to accelerate flame spread, the fact that rapid flame spread beneath a combustible ceiling is common in real fires is attributed to the additional external heating from the hot gas layer.

Figure 4: Total heat flux vs. distance from the center, normalised by flame radius

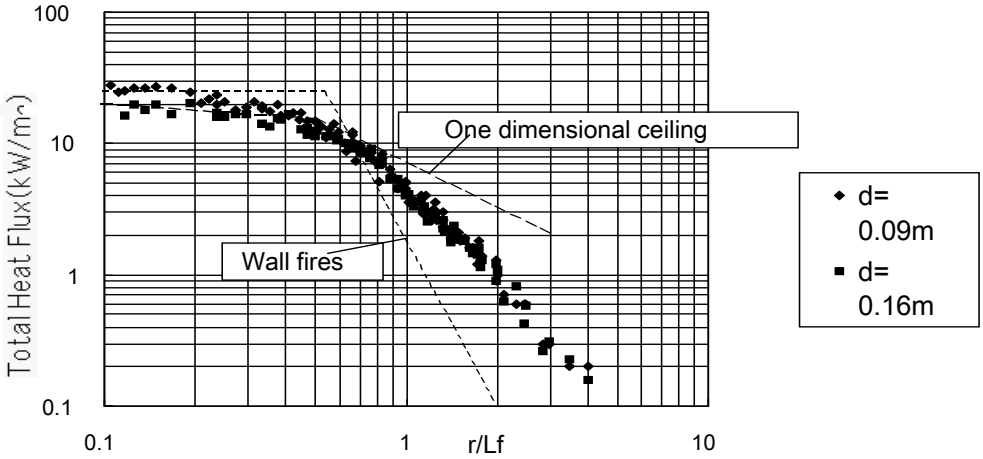

Dimensional relations for ceiling flames

A "first estimate" of the structure of ceiling flames can be made by introducing the main experimental relationships into the incompressible momentum equation, the energy equation and the continuity equation in the cylindrical coordinate:

$$\frac{\partial r\bar{v}_r\bar{v}_z}{\partial r}+\frac{\partial r\bar{v}_z^{\,2}}{\partial z}=-r\frac{\partial \bar{p}}{\partial z}-\frac{\partial r\overline{v_r' v_z'}}{\partial r}-\frac{\partial r\overline{v_z'^{\,2}}}{\partial z}-rg\beta\bar{\theta} \tag{1}$$

$$\frac{\partial r\bar{v}_r\bar{\theta}}{\partial r}+\frac{\partial r\bar{v}_z\bar{\theta}}{\partial z}=-\frac{\partial r\overline{v_r'\theta}}{\partial r}-\frac{\partial r\overline{v_z'\theta}}{\partial z}+\frac{r\bar{q}}{\rho C_p} \tag{2}$$

$$\frac{\partial r\bar{v}_r}{\partial r}+\frac{\partial r\bar{v}_z}{\partial z}=0 \tag{3}$$

where z is the vertical coordinate taken downward from the ceiling surface. In order to derive dimensional relations, Equations 1 and 2 are integrated with respect to z over (0,∞) as:

$$\frac{d}{dr}\int_0^\infty r\bar{v}_r\bar{v}_z dz+r[\bar{v}_z^{\,2}]_0^\infty=-r[\bar{p}]_0^\infty-\frac{d}{dr}\int_0^\infty r\overline{v_r' v_z'}dz-rg\beta\int_0^\infty\bar{\theta}dz \tag{4}$$

$$\frac{d}{dr}\int_0^\infty r\bar{v}_r\bar{\theta}dz + r[\bar{v}_z\bar{\theta}]_0^\infty = -\frac{d}{dr}\int_0^\infty r\overline{v_r'\theta'}dz + \int_0^\infty \frac{r\bar{q}}{\rho C_p}dz \tag{5}$$

where $\overline{v_z'^2} = \overline{v_z'\theta'} = 0$ is assumed at $z = 0$ and at $z\to\infty$. Further assuming uniform flame thickness and entrainment velocity at the lower surface of the flame and representing the maximum v_r, v_z, and $\bar{\theta}$ at each horizontal distance, r, as $AQ^{\mu 1}r^m$, $BQ^{\mu 1}$, $CQ^{\mu 2}$, velocity and temperature rise distributions are described as:

$$\bar{v}_r = AQ^{\mu 1}\cdot r^m V_r(z/Q^l), \bar{v}_z = BQ^{\mu 1}\cdot V_z(z/Q^l), \bar{\theta} = CQ^{\mu 2}\cdot\Theta(z/Q^l) \tag{6}$$

where $V_r(z/Q^l)$,$V_z(z/Q^l)$,and $\theta(z/Q^l)$ are velocity and temperature rise profiles with unity as the maximum. The power dependence of $\bar{v}_r$ and $\bar{v}_z$ on Q is assumed as identical from the continuity equation. The heat release rate per unit horizontal area within the flame can be assumed as constant, $\int_0^\infty \bar{q}dz$ =15.3 k W/m^2 from Figure 3. It is also assumed that $\bar{v}_z = 0$ at $z = 0$ and $\bar{\theta} = 0$ at $z\to\infty$. Hence Equations 4 and 5 are written in more concrete form as follows:

$$(m+1)r^m ABQ^{2\mu 1+l}\int_0^\infty V_r(z')V_z(z')dz' = -r[\bar{p}]_0^\infty - \frac{d}{dr}\int_0^\infty r\overline{v_r'v_z'}dz - rg\beta CQ^{\mu 2+l}\int_0^\infty\Theta(z')dz' \tag{7}$$

$$(m+1)r^m ACQ^{\mu 1+\mu 2+l}\int_0^\infty V_r(z')\Theta(z')dz' = -\frac{d}{dr}\int_0^\infty r\overline{v_r'\theta'}dz + \frac{r}{\rho C_p}\int_0^\infty \bar{q}dz \tag{8}$$

where $z' = z/Q^l$. The power constants, m, $\mu 1$, $\mu 2$ and l are determined as follows. Since the integrals in the left hand side and in the last term of the right hand side of Equations 7 and 8 are constant, the power of r on the left hand side, m, must be $m = 1$. Similarly, since the power of Q in each term of these equations must be identical and $\int_0^\infty \bar{q}dz$ is constant, $\mu 2 = 2\mu 1$ and $l = -3\mu 1$ are obtained. Assuming the constant maximum temperature at each distance, $CQ^{\mu 2} = const$, these powers are estimated as $\mu 1 = \mu 2 = l = 0$. There is not as yet any other experimental evidence supporting $\mu 1 = \mu 2 = 0$, but $l = 0$, in other words the independence of the flame sheet thickness on heat release rate is consistent with the visual observation during the experiments. Also, independence of maximum temperature rise within the solid flame on heat release rate sounds natural as the maximum temperature rise in a solid flame of any other previously reported configurations is independent of heat release rate[79]. Other parameters describing the velocity and temperature distributions in Equation 5, A,C,$V_r(z)$,$\Theta(z)$, can also be correlated to each other through Equations 7 and 8. Assuming the proportionality of heat release rate per unit horizontal area of a flame to the rate of oxygen supply, the source term in the energy equation yields:

$$\int_0^\infty r\bar{q}dz = \frac{\Delta Hc,_{O_2}C[O_2]}{\chi}\frac{d}{dr}\int_0^\infty r\bar{v}_r dz = \frac{2Ar\Delta Hc,_{O_2}C[O_2]}{\chi}\int_0^\infty V_r(z')dz' \tag{9}$$

Summarising Equation 8 for the parameter A yields:

$$A = \chi\int_0^\infty \bar{q}dz \Big/ 2\Delta Hc,_{O_2}C[O_2]\int_0^\infty V_r(z)dz\,,\; v_r = Ar\cdot V_r(z) \tag{10}$$

Considering the superiority of the convection to the turbulent transport within a developed ceiling flame, use of Equation 10 in Equation 8 leads to:

$$2rAC\int_0^\infty V_r(z)\Theta(z)dz \cong \frac{\Delta Hc,_{O_2}C[O_2]}{\rho C_p\chi}\frac{d}{dr}\int_0^\infty r\overline{v_r}dz = \frac{2Ar\Delta Hc,_{O_2}C[O_2]}{\rho C_p\chi}\int_0^\infty V_r(z)\,dz \tag{11}$$

Equation 11 can be summarised for C as:

$$C \cong \Delta Hc,_{O_2}C[O_2]\int_0^\infty V_r(z)dz \Big/ \rho C_p\chi\int_0^\infty V_r(z)\Theta(z)dz\ ,\ \theta = C\cdot\Theta(z) \tag{12}$$

Among many parameters in Equations 10 and 12, χ , excess air ratio, is difficult to measure directly. Hence Equations 10 and 12 are more rightly characterised as a relation to estimate excess air ratio of ceiling flames from the temperature and velocity measurements rather than that to calculate A or C from those parameters in the right hand sides of these formulae:

$$\int_0^\infty V_r(z)dz\ ,\int_0^\infty \Theta(z)dz$$

These are experimental parameters, which characterise the flame thickness as these have dimensions of length and are essentially larger by the increase of the visible flame thickness.

One-dimensional ceiling flames can be analysed in a similar way. The two dimensional momentum and energy equations lead to comparable forms to Equations 4 and 5 as:

$$\frac{d}{dx}\int_0^\infty \overline{u}\,\overline{w}dz + [\overline{w}^2]_0^\infty = -[p]_0^\infty - \frac{d}{dx}\int_0^\infty \overline{w'\theta'}dz - g\beta\int_0^\infty \overline{\theta}dz \tag{13}$$

$$\frac{d}{dx}\int_0^\infty \overline{u}\,\overline{\theta}dz + [\overline{w}\,\overline{\theta}]_0^\infty = -\frac{d}{dx}\int_0^\infty \overline{w'\theta'}dz + \int_0^\infty \frac{\overline{q}}{\rho C_p}dz \tag{14}$$

Assuming the functional form for the velocity and temperature distributions as:

$$\overline{u} = A'\cdot X^n U(z), \overline{w} = B'\cdot W(z), \overline{\theta} = C'\cdot\Theta'(z) \tag{15}$$

and uniform heat release rate per unit area over the whole flame, the power constant ,*n*, in Equation 15 is determined as *n* = 1. This again means proportionality of horizontal velocity to the distance from the source. Relations among *A'*, *C'*, *U*(*z*), and Θ '(*z*) are summarised in a similar way to the circular flames as:

$$A' = \chi\int_0^\infty \overline{q}dz \Big/ \Delta Hc,_{O_2}C[O_2]\int_0^\infty U(z)\,dz \quad \overline{u} = A'x\cdot U(z) \tag{16}$$

$$C' \cong \Delta Hc,_{O_2}C[O_2]\int_0^\infty U(z)\,dz \Big/ \rho C_p\chi\int_0^\infty U(z)\Theta'(z)dz \quad \overline{\theta} = C'\cdot\Theta(z) \tag{17}$$

Deterministic flame properties for a one dimensional ceiling flame sheet and a circular ceiling flame sheet are essentially described by Equations 16 and 17 and by Equations 10 and 12 respectively. Influence of the mode of flame propagation can be assessed by comparing these four equations.

Similarity between the forms of Equations 12 and 17 suggests similar ranges of temperature rise in one dimensional and circular ceiling flames. On the other hand, the coefficient for:

$$\chi \int_0^\infty \bar{q} dz \Big/ \Delta H_{c,O_2} C[O_2] \int_0^\infty V_r(z) dz$$

in Equation 15 is twice as large as that in Equation 10 and heat release rate per unit area is notably larger in one-dimensional flames than in circular flames. These facts suggest that either horizontal velocity or flame thickness is notably larger for one-dimensional flames than for circular flames.

CONCLUSIONS

The following conclusions can be drawn from the experiments and the analysis of the present study:

(1) The area covered by a ceiling flame sheet is proportional to the effective heat release rate. Heat release rate per unit area is significantly higher for one-dimensional ceiling fires than for circular fires.

(2) Maximum heat flux from circular ceiling flames to the ceiling surface does not reach 30 kW/m^2. This is comparable with that for a one-dimensional flame, and is clearly lower than surface heat flux from wall fires of similar heat input. This weak heat flux does not seem to be enough to cause rapid flame spread beneath the ceiling although rapid flame spread along a combustible ceiling is rather common in real and experimental fires. It suggests significance of the role of preheating from the fire source and overall heating of the ceiling by the smoke layer.

(3) Entrainment of air to a ceiling flame is believed to be uniform over a ceiling flame. Entrained air per unit area of flame is believed to be significantly greater in one-dimensional flames than in circular flames.

(4) Combustion efficiency in ceiling fires may become significantly lower than in upward turbulent flames.

(5) Dimensional analysis suggests proportionality of horizontal velocity in a circular ceiling flame to the distance from the center. It also suggests that either horizontal velocity or flame thickness is significantly greater in one-dimensional flames than in circular flames.

The present test configuration was clearly different from any realistic fires which normally do not starting from the ceiling. These observations should be examined against ceiling fires in more realistic room fire experiments, in which the physics is probably more complicated. It is also important to emphasise the necessity of further measurements of temperature and velocity fields in ceiling flames for the verification and improvement of the analysis discussed in this report.

ACKNOWLEDGMENTS

The authors wish to acknowledge efforts of Mr R. Takaike, Mr T. Yabuta, and Mr T. Kimura, formerly graduate students of Science University of Tokyo who assisted in the experiments.

NOMENCLATURE

A,A',B,B',C,C'	constants
$C[\,]$	mass concentration
C_p	specific heat of air
g	gravitational acceleration
$\Delta H_{C,O2}$	heat of combustion per unit mass of oxygen(13.17MJ/kg)
L_f:	flame length, flame radius
$l, m, n, \mu 1, \mu 2$	power constants
p	gauge pressure
Q	heat release rate
q	heat release rate per unit volume
q_T	total heat flux
r	radial distance
u	x-directional velocity in the Cartesian coordinate
v	velocity component in cylindrical coordinate
w	z-directional velocity in the Cartesian coordinate
x	downstream horizontal distance in the Cartesian coordinate
z	downward vertical distance in the Cartesian coordinate

Greek symbols

β	expansion coefficient
θ	excess temperature
ρ	density of air
χ	excess air ratio

Subscripts and other symbols:

l	per unit width
r	radial direction
z	vertical direction(downward)
$\bar{}$	Time averaging
$'$	eddy fluctuation

REFERENCES

1 Orloff, L., and de Ris, J.: Modeling of Ceiling Fires, Proceedings of the Fourteenth Symposium(Intern'l) on Combustion, p979- 992, 1971.

2. Babrauskas, V., Flame Lengths under Ceilings, Fire and Materials, 4, p119- 126, 1980.

3. Suzuki, T., Sekizawa, A., Satoh, H., Yamada, T., Yanai, E., Kurioka, H., and Kimura, Y., An Experimental Study of Ejected Flames of a High-rise Building – Effects of depth of balcony on ejected flames, Proceedings of the Fourth Asia-Oceania Symposium on Fire Science and Technology, p363- 374, Tokyo, 2000.

4. Thomas, P.H., Webster, C.T., Raftery, M.M., Some experiments on buoyant diffusion flames, Combustion and Flame, Vol.5, 1961.

5. Yokoi, S., On the Height of Flames, Bulletin of Japan Association for Fire Science and Engineering, Vol.13, No.1, 1963(in Japanese).

6. Cetegen, B., Zukoski, E.E., Kubota, T., Entrainment and Flame Geometry of Fire Plumes, NBS-GCR-82- 402, 1982.

7. Heskestad, G., Luminous heights of turbulent flames, Fire Safety Journal, Vol.5, 1983.

8. Hasemi, Y., Yoshida, M., Yokobayashi, S., Wakamatsu, Takao, Flame Heat Transfer and Concurrent Flame Spread in Ceiling Fire Configuration, Proceedings of the Fifth International Symposium on Fire Safety Science, Melbourne, 1997.

9. Hasemi, Y., Experimental Wall Flame Heat Transfer Correlations for the Analysis of Upward Wall Flame Spread, Fire Science and Technology, Vol.4, No.2, 1984.